Reliability and Safety Monitoring for more Electrical Transportation

B. Allard[1], G. Clerc[2], E. Dumitrescu[1], R. German[2], A. Lievre[2], M. Makdessi[2], E. Niel[1], R. Ouaida[2,3], R. Perrin[1], L. Piétrac[1], H. Razik[2], T. Santini[1,4], A. Sari[2], A. Soualhi[5], P. Venet[2]

1. Univ. Lyon, Ampere, INSA Lyon, France
2. Univ. Lyon, Ampere, Univ. Claude Bernard, France
3 : Thales Microelectronics, France
4 : Airbus Group Innovation, France
5. Univ.Lyon, LASPI, Univ. Saint Etienne, France

Abstract: Development of hybrid and electrical cars encounters integration of a key enabler. Integration, at the largest meaning, delivers a system that is greater than the sum of its parts. New technologies are considered and tight combinations of existing technologies are experimented. Evaluating the possibilities of failure mechanism, investigation reliability and the way for active safety monitoring are impacted as studies have to be revisited and new approaches are to be delivered. In this context, Ampere-lab is carrying several activities that are summarized here. Activities on high-temperature have led to analyses of failure mechanisms and possibility of reliability evaluation on wide-band-gap semiconductors. Passive devices receive new efforts as temperature ranges are pushed. Storage components become key devices with the idea to bring their lifetime to the limit. Prognostics and diagnostics are renewed issues.

Keywords: high temperature power conversion, wide-band-gap semiconductors, magnetic devices, dielectric devices, super capacitors, batteries, prognostics, diagnostics, and supervision of electrical network.

1. Introduction

Electrical vehicle, EV or HEV, is the ground for advanced developments in term of electrical network. Advances are comparable in diversity, constraints and objectives as the ones related to smart grids. An electrical network is an assembly of software and hardware components (Fig. 1, [1]). Different schematics may be appreciated depending on the issues to enlighten. In Figure 2, the network aspect is more obvious with the exchanges of information and energy between components.

Reliability of such a network is complex to evaluate and monitor. Each components of the network are subject to analyses in order to assess reliability indicators. Unfortunately the assembly of satisfying components in term of lifetime or reliability is not guarantee of system reliability. The assembly should follow a dedicated design approach for safety. In a second step the operation of the system should be monitored to assess the real conditions and their impact on the remaining lifetime of the system. Prognostic helps to build a map of targeted lifetime and diagnostic covers the assessment of realistic indicators under real mission profiles.

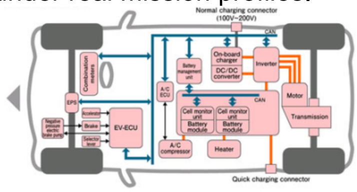

Figure 1: Possible schematic of the electrical network in an electrical vehicle [1]

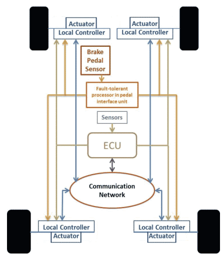

Figure 2: Example of brake-by-wire network point-of-view [2]

The paper summarizes several activities performed at Ampere-lab toward the reliability and safety assessment of embedded electrical network for electrical vehicles. Hierarchically and considering the traction issue, it may be seen that a power converter that comprises active and passive components while the energy is delivered from a battery system pilots the electrical motor.

High levels of cycling and high ambient temperature are generally stress factors. Wide band gap semiconductors are good candidates but suffer from several limitations. Section 2 details aging analyses and the proposal of a law for remaining useful lifetime evaluation. Active devices come with passive devices and Section 2 details some activities about reliability of capacitors and the behavior of air-core transformers for control signal isolation for drivers. Section 2 is dedicated to reliability of energy storage systems, a long-term activity at Ampere-lab. Diagnostics, prognostics and health monitoring approaches are given in Section 4. Finally several on-going results are detailed in Section 5 about design for safety of an electrical network.

2. Components of converters

2.1 Failure of SiC MOSFET gate oxide

When a silicon carbide MOSFET is submitted in switching conditions to a prolonged stress, there is no doubt that failure mechanisms will be triggered in time. In [3, 4] is detailed the analysis of failure mechanisms related to the gate of SiC MOSFET in harsh temperature environment. Ageing tests have been performed in stress switching conditions with a monitoring of device characteristics. Failures sensed from the gate (Fig. 3) have been investigated as detailed in [5].

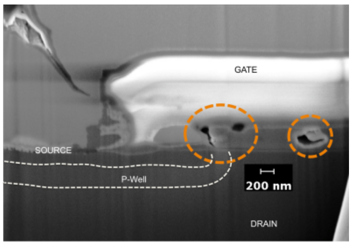

Figure 3: Cracks at gate level in a FIB image of a sample

2.2 Tentative remaining useful life evaluation

In relation to the previous study, the phenomenon of Threshold Voltage instability has been reported to be a critical issue for the first generations of commercial SiC MOSFETs. The long-term reliability of such device has to be estimated prior to any integration regarding electrical vehicle mission profiles [6].An approach based on the Acceleration Degradation Test methodology allows evaluating the time-to-failure, as well as its distribution, in nominal EV/HEV application from the data collected in accelerated conditions . Aging tests produce a set of data (like threshold voltage deviation in Fig. 4). All data are used to estimate the lifetime distribution in each test conditions. Ultimately these lifetime distributions are used to model voltage and thermal related acceleration factor and to extrapolate the time-to-failure in a given application. Due to the uncertainty and variability within devices, the deterioration process can be regarded as a time-dependent stochastic process.

Among the various existing stochastic process, the non-homogenous Gamma process could be a good candidate for modeling the degradation of SiC MOSFET threshold voltage.

The use of a gamma process in the field of reliability has been introduced in 1975 by M. Abdel-Hameed [8] to model gradual damage monotonically accumulating over time. Since then, it has been widely used for maintenance optimization models based on degradation data [9]. Nevertheless, as far as the authors know, the use of a non-homogeneous Gamma process to model the threshold voltage degradation of a commercial SiC MOSFET is original [7].

Let X(t) be the degradation level at time t and {X(t),t≥0} a non-homogeneous gamma process. Then the probability density function associated with the increment of degradation ($\Delta x = x_{t_i} - x_{t_{i-1}}$) is given by:

$$f_{\Delta X(t)}(\Delta x|\Delta v(t), u) = \frac{u^{\Delta v(t)}\, x^{\Delta v(t)-1}\, e^{-ux}}{\Gamma(\Delta v(t))} \quad (2)$$

Where x is the support of the distribution ($x \in [0; +\infty[$) , Γ(v) is the gamma Euler function $v(t)$ and u>0 are respectively a time-dependent shape parameter and a constant scale parameter.

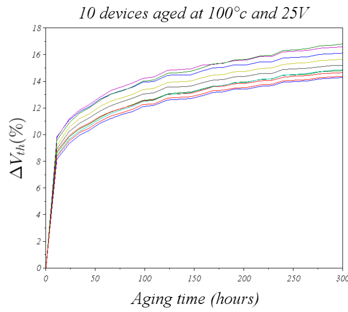

Figure 4: Threshold voltage variation as a function of aging time for V_{GS} = 25 V and T_j = 100 °C.Once the degradation process has been modeled it is possible to estimate the lifetime distribution associated to this V_{th} degradation. A component is said to fail when the deterioration level reaches a threshold limit D_f (a limit in threshold voltage value). Let T be the failure time. Due to the gamma distributed deterioration, the lifetime distribution F(t) can be written as:

$$F(t) = \Pr\{X(t) \geq D_f\} = \frac{\Gamma(v(t), D_f u)}{\Gamma(v(t))} \, (2)$$

Where $\Gamma(v(t), D_f u) = \int_{t=x}^{\infty} t^{a-1} e^{-t} dt$ is an incomplete gamma function for $x \geq 0$ and $a > 0$.

A simple algorithm is needed to populate the stochastic process, X.

Fig. 5 shows an example of lifetime distribution extracted from measurements of 3 V_{GS} conditions at Tj=50°C.

Using An Inverse-power law it is possible to express the voltage acceleration factor by:

$$AF(V, V_u) = \frac{L(V_u)}{L(V)} = \left(\frac{V}{V_u}\right)^{\beta} \quad (3)$$

Where V and T_u are respectively the gate voltage for acceleration test and nominal application expressed in volts.

Finally a corrected lifetime distribution is obtained incorporating the acceleration factors in order to assess the lifetime during normal operations.

Ultimately the Gamma process enables to evaluate the remaining useful life of the device in a first step toward prognostic of remaining useful life in embedded power electronics.

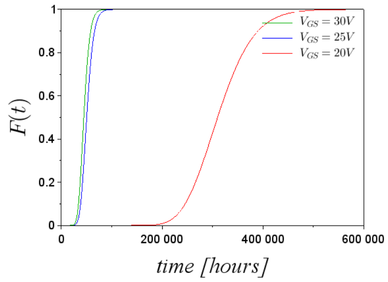

Figure 4: Lifetime distribution function for 3 V_{GS} ageing tests conditions at Tj =50°C

The Remaining Useful Life (RUL) of a device or a system is defined as the amount of time from the current instant to the End-of -Life (EOL) of the system. The RUL estimation is required for the implementation of condition-based maintenance (CBM) [9] and Prognostic and Health Monitoring (PHM) [10]. The approach carried out for RUL prognostic purpose is quite similar to the one used for TTF estimation. The parameters associated with the degradation process are estimated by maximizing the likelihood function. Then the degradation is extrapolated until it reaches the failure criterion (D_f, 20% deviation in our study) as presented in Fig. 5.

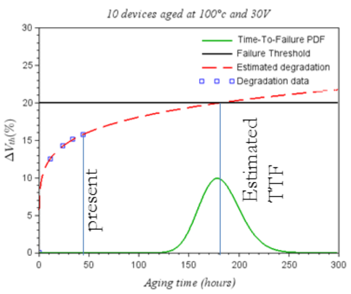

Figure 5: Time-To-Failure estimation and pdf associated at aging moment 49h

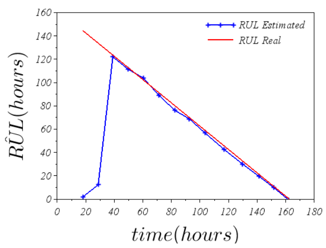

Figure 6: RUL estimation for different time during the ageing process

The same estimation is performed at different moments of the aging process. Thus the Remaining Useful Life is defined by the duration between the prognostic time and the estimated Time-To-Failure (Fig. 6). Given the SiC MOSFETs taken as example vehicles of the methodology, the very first estimation after 19h and 30h of test are very pessimistic compared to the real end of life (about 160h). These underestimations of the TTF in the first hours of tests are linked to the rapid increase of the Threshold voltage at the beginning of the aging process as observed in Fig. 4.

2.4 Reliability of air-core transformers

Air-core transformers are considered in the isolation of control signal at the input of drivers. In a previous paper, [11] endurance tests on the coreless chip had been performed at 200°C and an important degradations were observed. It was caused by oxidation of the insulation layer as no specific coating was used. In recent tests, the coreless chips have been coated with parylene and the preliminary results are presented in Fig.7.

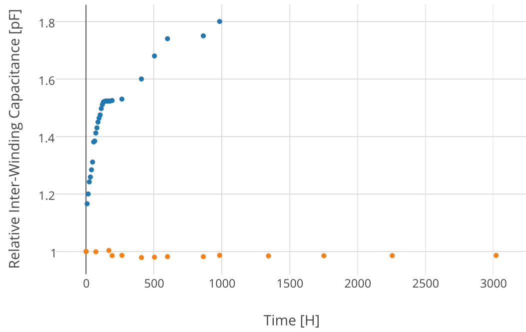

Figure 7: Relative Inter-winding capacitance evolution of coreless transformer with (red) and without (blue) parylene coating.

The parameter used to estimate the aging is the parasitic capacitance between the primary and the secondary windings of the coreless transformer. It can be observed that for coated transformer, there is no significant degradation. A preliminary conclusion is that the proposed coreless transformers withstand a temperature of 200°C. Currently, coreless transformers are tested in a control isolation application at 200°C with no issue.

2.5 Failure of capacitors and remaining useful life evaluation

Electrolytic and metallized film capacitors are among the most popular capacitors used in electronic equipment for automotive. The choice of capacitors is of major importance because one of the most frequent causes of the equipment breakdowns results from the failure of capacitors, and will therefore determine the overall lifetime of the system. During their operating lifetime, capacitors may be subject to a variety of stresses that can irreversibly degrade their properties with time and cause their so-called "ageing". Ageing mechanisms capacitors are quite well known for metallized film capacitors [12-14] and electrolytic capacitors [15].
Considering the simplified electrical model showed in Fig. 8, with ESR the Equivalent Series Resistance taking into account all losses in the component; ESL the equivalent series inductance due to the capacitors windings and electrodes and C the capacitance of the capacitor, ageing modes

capacitors result in an increase of ESR and/or a decrease of C.

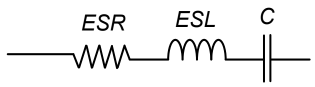

Figure 8: Simplified electrical model of capacitors

For example, to model natural random events such as self-healing phenomena (the main ageing mechanism) for metallized polypropylene film capacitor, the evolution of the capacitance C as a function of time t can be given by the equation below [13]:

$$C(t)=A+\lambda_1.\lambda_2.exp(-\lambda_1.t) \quad (4)$$

Where A is a parameter which depends on the capacitance initial value, and λ_1, λ_2 depend on the component characteristics and the applied stresses [13]. The adequacy of equation (4) with the capacitance evolution under different electrical and thermal stresses is shown in Fig. 9.

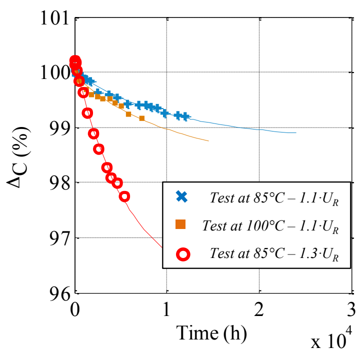

Figure 9: Comparison between the experimental values and the capacitance evolution model, U_R represents the capacitor rated voltage

For aluminum electrolytic capacitor, evaporation of electrolyte is the main cause of ageing. When the electrolyte evaporates, ESR increases significantly and capacitance C decreases. Several models describe ESR and C evolutions as a function of ageing time. For example, C(t) and ESR(t) for a given temperature can be given by:

$$C(t)=C_0-a_C.t \quad (5)$$

$$ESR(t)=ESR_0+a_R.t.exp(b_R.t) \quad (6)$$

ESR_0 and C_0 are the values of ESR and C for a healthy capacitor. The different coefficients a_R, b_R and a_C are functions of the component. They depend on the geometry of this latter, of its technological characteristics and of the utilized electrolyte. Considering the Arrhenius model in (3), we can deduce the evolution of the parameters of this model as a function of time for another temperature. The activation energy E_a of Arrhenius model was estimated at 0.4 eV.

Since the drifts of the different parameters are known and can be expressed as equations, predictive maintenance systems of capacitors can be elaborated [16].

3. Energy storage

3.1 Ageing mechanisms in supercapacitors

The reliability and diagnostic of state of health of different energy storage components are a major issue. Supercapacitors (SC) and batteries impedance monitoring is mainly used as a non-destructive test for ageing monitoring. Our work concern lithium-ion and lead-acid batteries and supercapacitors. In this part, we do a focus on SC.

For storage energy in SC, electronic charges are maintained face to face with ionic electrolytic counter charges by electrostatic forces in two space charges zones of nanometer scale (zone 1 and 3 in Fig. 10), this phenomenon is called double layer. Other electrolyte zone (zone 2) stays electrically neutral. The energy storage capacity is proportional to the face-to-face surface so the SC electrodes are constituted by porous material (activated carbon more commonly).

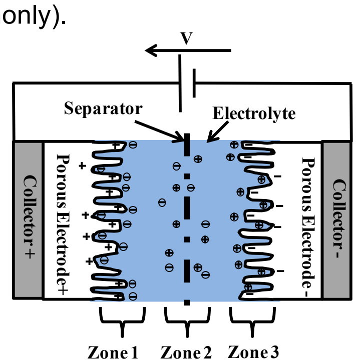

Figure 10 : Constitution and energy storage principle for SC

In electrochemical energy storage system, it is usual to use Nyquist diagram for shown the impedance of components. Fig. 11 presents the impedance spectrum of a 3000F SC obtained by electrochemical impedance spectroscopy (EIS). The low frequency part of the spectrum (I) is associated with the capacitive energy storage. The second zone (II) corresponds to the zone in which energy storage doesn't occur. Inductive phenomena start to occur because of the wire-wounded geometry of components [17-18].

As any electric energy storage system, supercapacitors have a limited lifetime. Indeed, they damage with time because of parasitic reactions between electrodes and electrolyte. Porous electrodes are complex structures and pores present size dispersion because of manufacturing processes.

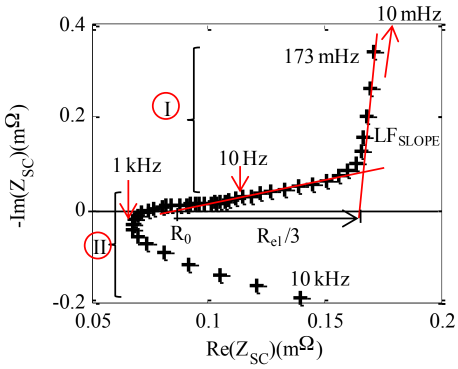

Figure 11: SC Impedance spectrum for a 3000F SC

As a matter of fact, SCs behavior is dependent on various parameters such as pore size distribution of electrodes, electrolyte state, temperature, and aging… We have developed multi-pore (MP) model of supercapacitor taking into account physical considerations. This model allows analyzing the behavior of supercapacitor in its whole operating frequency range by modeling each group of electrode pores as a branch of an electrical equivalent circuit. It is possible to study the specific impact of ageing on supercapacitor through different pore groups thanks to multi-pore model. Each group of pores is represented as a parallel branch on the equivalent circuit as shown in Fig. 12. Impedance of the global MP porous structure is thus composed with several branches as depicted in Fig. 13.

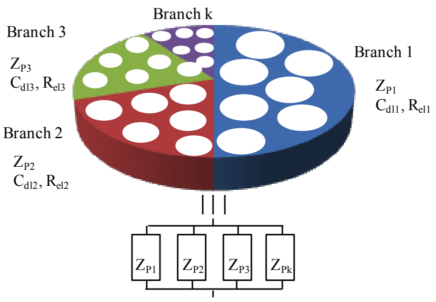

Figure 12: Principle of MP model

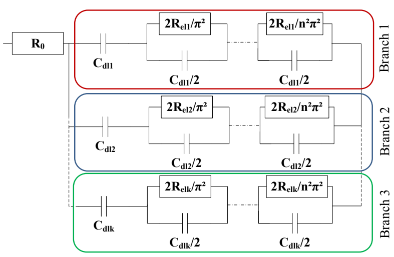

Figure 13: MP model equivalent circuit

As depicted in Figs. 14, a three-branches MP model is very accurate to model the impedance behavior of the SC throughout more than 3 decades. The measurement frequency range includes the normal frequency range of SCs usage.

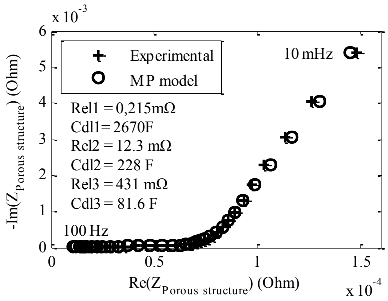

Figure 14: Fitting of MP model with experimental SC

As said before, highly reactive parasitic functional groups present on electrode surface, porous structure slowly blocks with parasitic reactions products (solids and gases) as shown in Fig. 15.

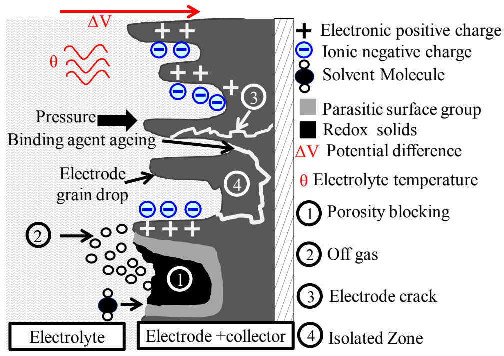

Figure 15: Ageing mechanisms for SC

All of SC ageing phenomena increase the Equivalent Series Resistance (ESR) and decrease the capacitance C of the porous structure as shown in Fig. 16 representing SC impedance evolution with time.

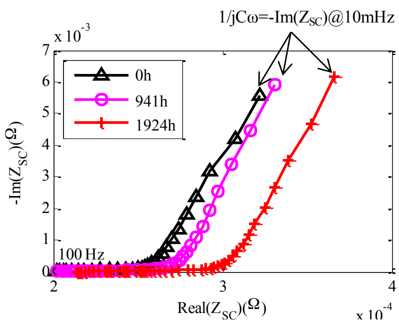

Figure 16: Impact of ageing on SC impedance

MP model can be a powerful tool for SC aging monitoring. The advantage of MP model compared to others is that it allows following the evolution of different pore groups. Many parameters change during aging: the pore accessibility resistance (Reli) to electrolyte (i.e. pore length), the branch capacitances (i.e. storage surface), ions diameter (solvation), thickness of double layer, etc. That allows to explain the different process acting during ageing and to monitor the latter parameters (Fig. 17). More information on MP aging monitoring can be found in [19].

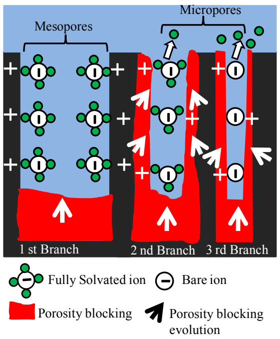

Figure 17: Deduced effects of ageing on branches

In power network, supercapacitors are subject to high frequencies current ripple due to the presence of DC-DC converters. We have studied they are a factor of overageing for supercapacitors. The results show that high frequency current ripples are transparent in term of ageing. These results are interesting as they prove that the supercapacitors can be inserted in polluted power networks without particular precautions [20].

3.2 Supercapacitor remaining useful life evaluation

Two types of ageing may occur in supercapacitor failure: floating ageing (constant voltage and temperature constraints) and cycling ageing (high current charge/ discharge cycles).

.

For floating ageing, the kinetic of supercapacitor ageing depends essentially on temperature and voltage. Floating degradation law can be obtained thanks to Eyring law that generalizes Arrhenius model on several parameters other than temperature (here the voltage parameter is added). It is an ageing law able to predict the lifetime of a system as a function of constraints level (U_{SC} voltage, temperature T), a known lifetime for voltage U_{SC1} and temperature T_1 constraints. It can be expressed as follow [21]:

$$t_{life}(T, U_{SC}) = t_{life}(T_1; U_{SC1}).A_{FU_{sc}}^{\left(\frac{-(U_{SC}-U_{SC1})}{\Delta U_{SC}}\right)}.A_{FT}^{\left(\frac{-(T-T_1)}{\Delta T}\right)} \quad (7)$$

A_{FUsc} and A_{FT} are respectively called voltage and temperature acceleration factors. They are the quantifiers of ageing constraints impact. We can notice than both acceleration factors are linked with a differential value (ΔU_{SC} and ΔT). A value of 2 for A_{FUsc} or A_{FT} means that the failure appearance time is divided by 2 every time the constraint level is increased by ΔU_{SC} or ΔT.

For example, Fig. 10 presents the experimental ageing results (capacitance decrease) for 60 °C temperature for different voltage constraints. We can calculate A_{FUsc} (1.8 for ΔU_{SC}=0.1 V) and A_{FT} (2.1 for ΔT=10 °C) [20].

For cycling ageing, the charge/discharge current heats the supercapacitor. The consideration of this heating in the equation (7) is not sufficient. Indeed, besides self-heating of the component, the current creates a significant acceleration of ageing which must be taken into account. In [22] a law considering I_{RMS} current was proposed:

$$t_{life} = t_{life}(T_1; U_{SC1}, I_{RMS1}) A_{FU_{sc}}^{\left(\frac{-(U_{SC}-U_{SC1})}{\Delta U_{SC}}\right)} A_{FT}^{\left(\frac{-(T-T_1)}{\Delta T}\right)} A_{FI_{RMS}}^{\left(\frac{-(I_{RMS}-I_{RMS1})}{\Delta I_{RMS}}\right)} \quad (8)$$

with RMS current acceleration factors A_{FIRMS} = 2 for ΔI_{RMS}=30 A.

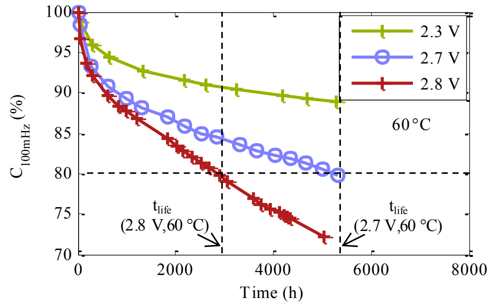

Figure 18 Presentation of ageing results and lifetime extraction

Nevertheless, the biggest issue of this method is that it does not allow estimating the shape of capacitance decrease with time. Thus, we take interest in ageing laws able to give the capacitance value with time.

The loss of capacitance is mainly influenced by the growth of one solid layer between the electrode and electrolyte was proposed. The increase in interface layer thickness is often represented by a law proportional to the square root of time (t). This model is quite well known for describing batteries ageing. By considering that the loss of capacitance is proportional to the growth of solid electrolyte interface, we can express the loss of capacitance as follow:

$$\Delta C_{100mHz}(t) = A_C \cdot \sqrt{t} \quad (9)$$

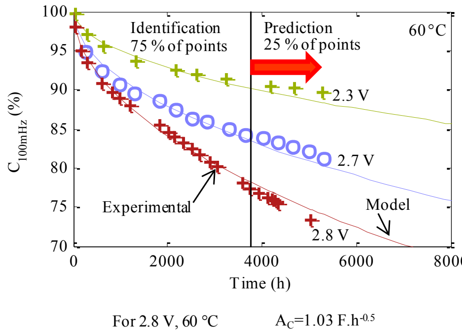

Figure 19: Decrease in C_{100mHz} (in percent) compared with model

Comparisons between experimental results and this law are presented in Fig. 19. The model parameters are extracted on 75% of the experimental points (identification zone) with a simple nonlinear least squares method minimizing the difference between (9) and the experimental capacitance decrease with time.. The extracted parameters for 2.8 V, 60 °C are given as example in the figure. Then the model and the 25% remaining experimental points are compared (prediction zone).

3.3 Estimation of lithium ion battery state of health

Estimation of lithium ion battery state of health depends on the type of vehicle. For electric vehicle, the state of health is defined by considering the battery capacity. This case is not discussed in this paper.

In hybrid vehicles, lithium-ion cells constituting a battery pack are frequently used to provide and recover high power in order to assist the vehicle's internal combustion engine powertrain. This usage is more present in mild hybrid applications where the battery does not have long discharge time. In such conditions, the pack's series resistance R_S proved to be an important parameter to monitor. This resistance, monitored by the Battery Management System (BMS), reflecting the available power level in the cell can be used as an indicator to enhance the security of the battery pack. Its evolution is also used to quantify its ageing (State of Health).

The cells series resistance can be usually identified through the voltage drop occurring across the cell caused by a high current variation profile (mild hybrid conditions). The calculation of $R_{\Delta V/\Delta I}$ is based on the voltage drops when current variations reach a certain value. The following formula is adopted:

$$R_{\Delta V/\Delta I} = \Delta V_{cell} / \Delta I_{cell} \quad (10)$$

The determination of resistance at each current variation may be inaccurate and/or noisy. This inaccuracy increases with the variations between successive iterations. Monitoring the resistance must be "filtered" and one method than we propose is to accomplish it through an "exponential moving average" method. It offers the advantage of a minimum storage space (no need to save the previous samples) and a low computing power, which is an advantage for BMS:

With the exponential moving average, the resistance average R_{S_k} is updated with each new measurement of $R_{\Delta V/\Delta I}$, which is our value to filter.

$$R_{S_k} = R_{S_{k-1}} . (1 - \alpha \ ) + R_{\Delta V/\Delta I} . \alpha \quad (11)$$

The level of previous samples taken into account is performed through a coefficient α. This coefficient, chosen between 0 and 1, modulates the new sample compared to the previous average that includes the effect of previous samples. The determination of α is detailed in [23].

In Fig. 20, series resistance R_S determination is represented with a 20 minutes current profile that simulates mild hybrid utilization for a single cell (nominal capacity of 11.5 Ah).

With different coefficients α, we can see the filtering effect that introduces a delay in the determination, but provides a more steady response. Some compromises therefore allow satisfying results while maintaining a good calculation close to real time considering the operation mode.

This approach provides good results for mild hybrid conditions, while minimizing the computing power required.

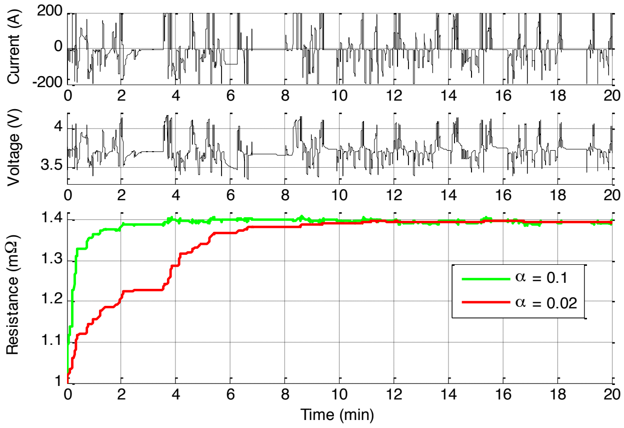

Figure 20: Determining the average series resistance from incorrect initialization: 1 mΩ

4. From diagnostics to prognostics

Research activities increasing the lifetime of complex systems go through the knowledge of physical phenomena or logical propagation defects. Investigation fields include defect identification, diagnosis and safe methods of design and fault tolerance. Applications, which deal with electric drives, actuator (motor, bearings), electrical drives and storage elements (eg super capacitors), are in constant evolution. Since these devices are widely used in applications dealing with automotive as more electric airplane, it is important to monitor and track their ageing. Moreover, a novel approach has recently been proposed to predict the ageing of ball bearings, induction motors and super capacitors. The challenge to overcome is the Remaining Useful Lifetime of all these components. For that purpose, a neo-fuzzy neural network has been developed in our laboratory.

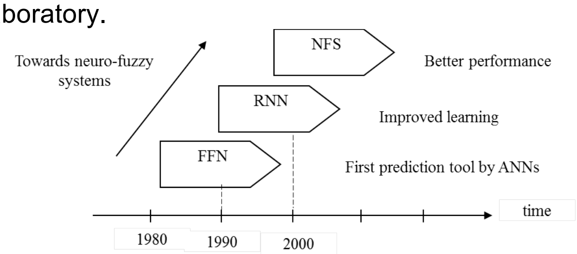

Figure 21: Applications of ANNs for the prediction.

This method is based on the analysis of recorded data, in order to realize a prognosis or a diagnostic of the device under test. Among all Artificial Neural Network (ANN) applications from 1980 to now, we can see that two types of network have been raised up: the Feed Forward Neural Networks (FFNN) and the recurrent neural networks (RNN)[24-26].

However, Neural Networks need a training process and they are composed inside the network of a large number of non-linear functions. It is why some authors describe it as a black box.

4.1 Neo-Fuzzy Neurons

In order to make a long-term predictor for diagnosis purpose, a Neo-Fuzzy Neurons (NFN) developed by Dr Rivas has retained our attention. Together, we gave birth to an association of 2 structures based on the fuzzy logic and the neural network. The Neo-fuzzy Neurons predictor is composed of membership functions for all inputs and the output system is composed of a layer using sigmoid functions for example. The structure of this long-term predictor with n inputs and one1output is shown in Fig. 22.

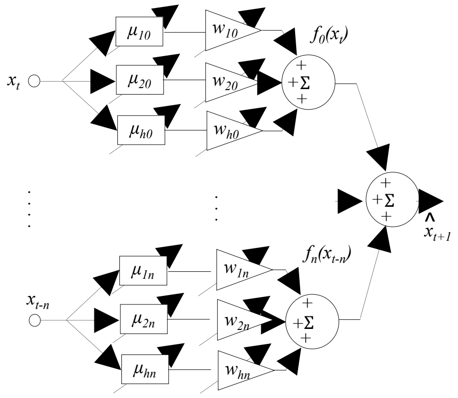

Figure 22: One-step-ahead prediction by the NFN predictor.

The output of the NFN predictor is expressed as follows

$$\hat{x}_{t+1} = \sum_{i=0}^{n} f_i(x_{t-i}) \qquad (12)$$

Where x_{t-i} is the i-th input i={0,1,…,n}, $\hat{x}_{t+1}$ is the system output which represents the prediction at time t+1.

The structural blocks of the neo-fuzzy neurons of the hidden layer, are nonlinear synapses based on:

$$\hat{x}_{t-i} = \sum_{j=1}^{h} w_{ji} . \mu_{ji}(x_{t-i}) \qquad (13)$$

Where w_{ji} are weights and $\mu_{ji}(x_{t-i})$ is the membership value.

Basically, membership functions are triangular functions. Fig. 23 shows these functions that are as follow:

$$\mu_{ji}(x_{t-i}) = \begin{cases} \frac{x_{t-i}-c_{j-1,i}}{c_{ji}-c_{j-1,i}} & if\ x_{t-i} \in [c_{j-1,i}, c_i] \\ \frac{c_{j+1,i}-x_{t-i}}{c_{j+1,i}-c_{ji}} & if\ x_{t-i} \in [c_{ji}, c_{j+1,i}] \\ 0 & otherwise \end{cases} \qquad (14)$$

Weights w_{ji} are updated during the training process thanks to databases. The worldwide approach is the incremental updating learning algorithm described as follows:

$$w_{ji} = -\rho(\hat{x}_{t+i} - x_{t-i})\mu_{ji}(x_{t-i}) \qquad (15)$$

Where ρ is the learning rate and x_{t+1} is the desired output at time t+1. As a consequence, a long-term prediction could be evaluated using this NFN at time t+p as follows:

$$\hat{x}_{t+p} = f_0(x_t) + \cdots + f_i(x_{t-i}) + \cdots + f_n(x_{t-n}) \qquad (16)$$

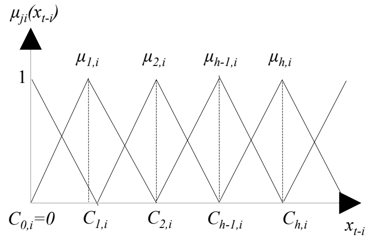

Figure 23: Triangular membership functions.

4.2 Experimental Results on super capacitor

The experimental platform used super capacitors (3000F, 2.7V) placed in a programmable precision incubator for applying the temperature constraints [27]. They are aged by groups of three at the same voltage conditions (2.8V for the first group, 2.7V and 2.3V for the third group) and at the same temperature (60°C). One can notice that the dispersion between the SC aging states in the same group is insignificant. All components are characterized regularly by using an impedance spectrometer.

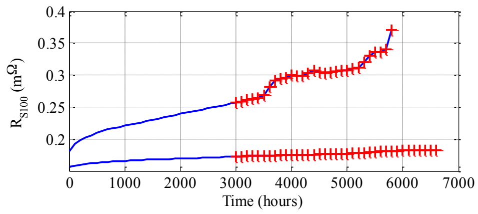

Figure 24: Training and validation of C_{dl} by the NFN predictor for accelerated calendar ageing test of SC1 (2.3V, 60°C) and SC3 (2.3V, 60°C).

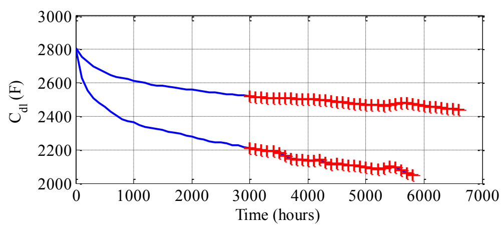

Figure 25: Training and validation of R_{S100} by the NFN predictor for accelerated calendar ageing test of SC1 (2.3V, 60°C) and SC3 (2.3V, 60°C).

After the data acquisition process, the serial resistance R_{S100} (R_{S100} is defined as the real part of SC impedance at 100mHz) and the double layer capacitance C_{dl} of the components SC1 at 2.3 V and SC3 at 2.8V will be obtained. These parameters and their corresponding voltages and temperatures will be used as inputs to train the NFN predictor. Two NFN models are defined. The inputs of the first one includes the current voltage, temperature and the time series of the serial resistance with V_t=2.7V and 2.8V, T_t=60°C, r =100 (r denotes the prediction step)

and n=7 (n defines the number of previous time steps). The inputs of the second one include the current voltage, temperature and the time series of the double layer capacitance.
Fig. 24 and 25 perform the training and validation results of the NFN predictor for R_{S100} and C_{dl} for components SC1 and SC3. Results show the efficiency of the proposed approach for the prognosis of SCs.

4.3 Experimental Results on Ball Bearings defects
This NFN predictor was applied in a real system to predict the trending data of bearings provided by the Center for Intelligent Maintenance Systems, University of Cincinnati. The test rig is composed of four Rexnord ZA-2115 double-row bearings installed on one shaft. The rotation speed was kept constant at 2000 rpm with 6000 lb radial load placed onto the shaft and bearing by a spring mechanism. The Root mean square (RMS) extracted from bearing vibration signals is worldwide considered excellent parameter for tracking the evolution of bearing condition. The RMS of the vibration signal of bearing 1, 2, 3 and 4 was recorded during 35 days in 2003 (Fig. 26). The vibration data of the bearing 4 are used to evaluate the performance of the ANFIS and the NFN for the prediction of its trending data. Vibration data of bearings 1, 2 and 3 are available and are used to identify the parameters of ANFIS and the NFN predictor [28]. The prediction of the future condition of the test bearing 4 consists of two steps: off-line and on-line. In the off-line step, the vibration data of the bearing 1, 2 and 3 are used to train the ANFIS and NFNN predictor. In the on-line step, the RMS of the vibration data of the test bearing 4 is used as inputs in the ANFIS and the NFNN predictor in order to predict the future values.

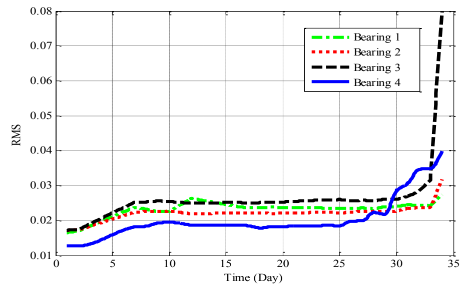

Figure 26: RMS of bearing 1, 2, 3 and 4.

In order to predict the evolution of the bearing 4, vibration data of the first 8 days of this bearing are used to train the methods: ANFIS and NFN predictor. This is made in addition to parameters of these predictor obtained for bearings 1 to 3 during the training process.
The results coming from the predictors (ANFIS and NFN) applied to the bearing 4 are shown in Fig. 27. As we can see, the result is better in term of faraway prediction by using the NFN predictor in comparison with the ANFIS predictor. This is the opposite conclusion in terms of nearest prediction.
In conclusion, the obtained results show the efficiency of both the proposed approach for the prognosis and for the tracking of the evolution of bearing conditions and the super capacitors.

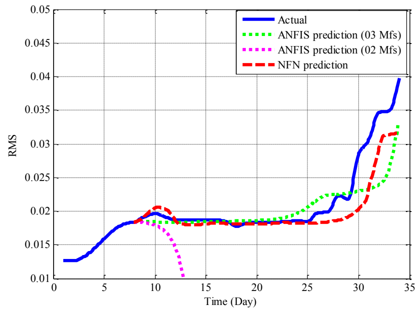

Figure 27: Predicted results of ANFIS and NFNN

5. Supervision and design for safety

5.1 Operating mode management
To ensure safety of a system subject to breakdowns, it is not only necessary to diagnose or predict failures, but the control of this system has also to react to faults. For an electrical vehicle, the safest response is usually to quickly stop the vehicle. However, this implies a lower availability. Another way to manage safety while ensuring greater availability is to use fault tolerance techniques such as isolation (performs the exclusion of the faulty component) or reconfiguration (reassigns tasks among non-failed components) [30]. When the system includes several components, a failure of one or more of them may leave the system in a degraded mode that offers only a subset of services to the user. To the extent that several components can fail, it becomes necessary to define a management modes policy. This management allows defining several degraded modes as well as several nominal modes. A mode is defined by a set of used components and by a set of requirements. For example, various nominal driving modes are available in up-market cars: normal, comfort, eco, sport... In each of these modes, all necessary components (engine, suspension, steering...) are available but aren't controlled in the same way according to different requirements. In case of damage of the performance of power steering or suspension system a degraded mode of conduct, with reduced speeds, ensures the availability of the vehicle while ensuring the safety of passengers. Formally, components and requirements are modeled with automata [31] and the behavior is studied with the point of view of event sequences. The approach is primarily based on individual study of each mode, starting with nominal modes, to ensure controllability and non-blocking for each one. The real difficulty is to study the mode changes to

verify the feasibility of these changing requirements including their physical feasibility. In fact, the state of common components can prevent instantaneous change and require a transient mode in which the state of these components is adapted to the new requirements. Various properties have been formalized [32] in order to detect possible problems of transition from mode 1 to mode 2, and those related to possible return to mode 1 after a time in mode 2.

5.2 Dynamic dependability assessment for distributed systems

Dynamic dependability notions have gained popularity as an efficient indicator to assess performance degradation during system life. Time dependent failure rates, as well as impact of operating constraints (for corrective even predictive maintenance), can no longer be ignored when characterizing service efficiency (cost/benefits, know-how, technologic engineering). In this way, factors influencing reference failure rates are restore rate have been discussed and computations are available based on simulation tools. The attempted results concern dimensioning as well as structural and functional design on one hand. Fault tolerance ability and real time reconfiguration would be also established and human management on the other hand.

The innovation investigation involves exploring a formal approach that integrates the effect of system life factors as maintenance means on associated components. This approach overcomes the drawbacks of pure probability oriented methods and error-prone apprehension on a global level. It also benefits from the inherent advantages of encapsulated capability of the formal techniques retained. Embedded formalism has been developed to model two important elements of dynamic reliability, namely component disturbance due to time and operating conditions. These impact the availability of the expected service on a global level. Therefore, innovative local dependency calculus has been introduced to model the dynamic reliability of the component subject to environmental constraints. High-level Petri nets have been used [29] on one hand to compose this coupling paradigm, and on the other hand to assess the dynamic reliability level for resources (local) and to compute the risk of service loss (global).

5.3 Component-based design of control-command systems

Due to design constraints bounding delays, costs and engineering resources, component re-usability has become a key issue in embedded systems' design. The expertise of the design process has shifted from code writing to the efficient management of Commercial-off-the-Shelf (COTS) libraries: by assembling adequately COTS components new functions can be quickly built. Yet by assembling COTS that have been separately designed, the resulting interactions cannot be entirely anticipated. Unwanted global behaviors may occur, although each component taken separately is considered free of errors.

This is why ensuring a safe behavior of a COTS-based system remains an important challenge. It calls for safe design methods and techniques, ensuring functional correctness.

Besides simulation, the model checking technique [33] is vital for discovering subtle bugs, often difficult to uncover by simulation. This technique is mature, yet designers must correct errors manually. This process is extremely tedious. It takes time, requires high-level expertise and deep insight in the design at hand. At any rate by attempting to manually correct an error, another one can be introduced, what creates a vicious circle.

This contribution provides a novel design method [35] based on the synergy between the Discrete Controller Synthesis (DCS) [34] and formal verification techniques. The main challenge is the automatic generation of correct-by-construction control-command COTS-based designs.

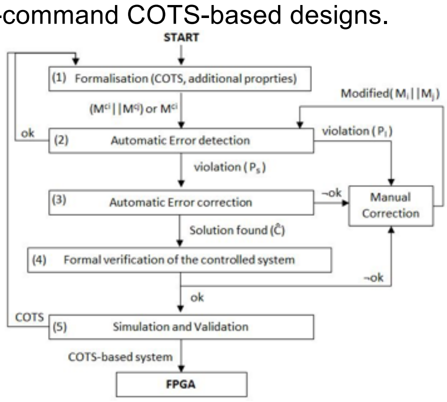

Figure 28: Safe COTS-based design method

In this context, COTS are designed using *ControlBuild*, according to a synchronous modeling paradigm. According to Fig. 28, COTS are assembled in order to meet functional specifications (Step 1). The assembly result is formally verified (Step 2), in order to assess the satisfaction of the specifications. If the verification is successful, then the design process continues; otherwise, a correcting patch generation is attempted, by using DCS (Step 3). The patch generation produces a logic component that constrains the behavior of the COTS assembly so that the desired functional requirement holds in the end. This controller is subsequently verified (Step 4) to ensure no behavioral incompatibilities exist with other valid functional requirements.

This method has been assessed on a simple yet expressive example: a passenger access system composed of two COTS: a door management and a filling-gap management COTS. This composition should satisfy a safety requirement: for passenger safety reasons, the doors should not open as long as the filling gap has not been fully deployed. This is expressed into the property specification language (PSL) standard: P = always (req_open → ack_deployed before ack_open).

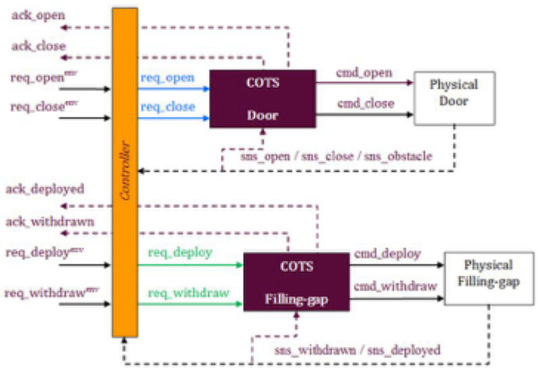

Figure 29: Enforcing a functional requirement P by DCS

The formal verification of P (Step 2) establishes its violation. DCS is used (Step 3) to generate a controller that is composed of the door and filling-gap COTS, and guarantees the satisfaction of P. The resulting controlled system is shown in Fig. 29.

Figure 30: simulation of the controlled system

In Fig. 30, simulation shows that at time 10s the driver requests to open the door (req_open^{env}) while the filling-gap is not yet deployed. The controller blocks this request (req_open) until second 31 where the filling-gap sensor (sns_deployed) provides the "full deploy" information; from that moment the controller stops blocking the door opening request. Regardless of the order in which the driver requests the doors and filling gap operations, they always operate in the safe order, according to P. The resulting architecture is ready for further simulation if desired, and for RTL synthesis.

6. Conclusion

Failure mode analyses, reliability, safety, diagnostics and prognostics, health-monitoring cover among other issues, a wide and interdisciplinary field. The paper wishes to illustrate some of the approaches where Ampere-lab brings contributions with respect to challenges in more-electrical transportation.

7. References

[1] [Available] http://johndayautomotivelectronics.com/tag/plug-in-parallel-hybrid/

[2] Abhishek Ramesh: "*Brake by wire*", Clemson University vehicular electronics laboratory, [Available] http://www.cvel.clemson.edu/auto

[3] R. Ouaida: "*Vieillissement et mécanismes de degradation pour des modules de puissance embarquant des composants SiC dans des environnement haute temperature*", PhD dissertation, INSA Lyon, 2014.

[4] R. Ouaida, R., M. Berthou, J. Leon, J., X. Perpina, S. Oge, S., P. Brosselard, C. Joubert: "*Gate Oxide Degradation of SiC MOSFET in Switching Conditions*," IEEE Electron Device Letters, 35 (12), 2014

[5] G. Peyresoubes: "*Understanding SiC Mosfet Reliability Issues under Harsh Environment switching Conditions Remains a Challenge*", APE (Paris) 2015

[6] T. Santini et al: "*Accelerated Degradation data of SiC MOSFETs for Lifetime and Remaining Useful Life Assessment*", European Symposium on Reliability of Electron Devices, ESREF, Berlin, 2014

[7] J. Lawless and M. Crowder: "*Covariates and random effects in a gamma process model with application to degradation and failure*," Lifetime Data Analysis, 10, 2004.

[8] M. Abdel-Hameed: "*A Gamma Wear Process*," IEEE Transactions on Reliability, 24, 1975

[9] J. Van Noortwijk: "*A survey of the application of gamma processes in maintenance*," Reliability of Engineering and System Safety, 2 (21), 2009

[10] M. Pecht: "*Prognostics and Health Management of Electronics*", New-York: John Wiley & Sons, 2008

[11] D. Bergogne et al: "*Integrated coreless transformer for high temperatures design and evaluation*", In 15th European Conference Power Electronics and Applications (EPE), 2013

[12] L. Hua, C. Yaohong, L. Fuchang, P. Bo, L. Fei, Z. Miao, et al., "*The capacitance loss mechanism of metallized film capacitor under pulsed discharge condition*," Dielectrics and Electrical Insulation, IEEE Transactions on, vol. 18, pp. 2089-2094, 2011.

[13] M. Makdessi, A. Sari, P. Venet, "*Metallized polymer film capacitors ageing law based on capacitance degradation*", Microelectronics Reliability, Vol. 54, Issues 9-10, Sept.-Oct. 2014.

[14] M. Makdessi, A. Sari, P. Venet, P. Bevilacqua, C. Joubert, "*Accelerated Ageing of Metallized Film Capacitors under High Ripple Currents Combined with a DC Voltage*" IEEE Transactions on Power Electronics, Vol. 30, n°5, May 2015.

[15] J. Martinez-Vega "*Dielectric Materials for Electrical Engineering*" - Chapter 18 P. Venet "Electrolytic capacitors", Publisher John Wiley & Sons Inc, 2010

[16] P. Venet, F. Perisse, M.H. El-Husseini, G. Rojat "*Realization of a Smart Electrolytic Capacitor Circuit*." IEEE Industrial Applications Magazine, vol. 8, n°1, January/February 2002.

[17] R. D. Levie, "*Electrochemical response of porous and rough electrodes, Advances in electrochemistry and Electrochemical Engineering*", Wiley Intersci., vol. 6, pp. 329–397, 1967.

[18] R. German, P. Venet, A. Sari, O. Briat, and J.-M. Vinassa, "Comparison of EDLC impedance models used for ageing monitoring", in Renewable Energies and Vehicular Technology (REVET), 2012 First International Conference on, march 2012, pp. 224 –229.

[19] R. German, P. Venet, A. Sari, O. Briat, and J.-M. Vinassa, "*Improved Supercapacitor Floating Ageing Interpretation Through Multipore Impedance Model Parameters Evolution*", IEEE Trans. Power Electron., vol. 29, no. 7, pp. 3669–3678, Jul. 2014.

[20] R. German, O. Briat, A. Sari, P. Venet, M. Ayadi, Y. Zitouni, and J. Vinassa, "*Impact of high frequency current ripple on supercapacitors ageing through floating ageing tests*", Microelectronics Reliability, vol. 53, no. 9-11, pp. 1643 – 1647, 2013.

[21] R. German, A. Sari, P. Venet, Y. Zitouni, O. Briat, J. M. Vinassa "*Ageing law for supercapacitors floating ageing*" 23rd IEEE International Symposium on Industrial Electronics, ISIE 2014.

[22] P. Kreczanik, P. Venet, A. Hijazi, G. Clerc, "*Study of supercapacitor ageing and lifetime estimation according to voltage, temperature and RMS current*", IEEE Transactions on Industrial Electronics, Vol. 61, Issue 9, Sept. 2014.

[23] A. Lievre; A. Sari, P. Venet, A. Hijazi, M. Ouattara-Brigaudet, S. Pelissier "*Practical Online Estimation of Lithium-Ion Batteries Apparent Series Resistance for Mild Hybrid Vehicles*", IEEE Trans. on Veh. Tech., to be published, 2015.

[24] Yamakawa T., Uchino E., Miki T., Kusanagi H.: "*A neo fuzzy neuron and its applications to system identification and prediction of the system behavior*", Int. Conf. on Fuzzy Logic and Neural Networks "LIZUKA–92". Lizuka, Japan, 1992

[25] Uchino E., Yamakawa T.: "*Soft computing based signal prediction, restoration and filtering Intelligent Hybrid Systems: Fuzzy Logic, Neural Networks and Genetic Algorithms*". Boston: Kluwer Academic Publisher, 1997

[26] Miki T., Yamakawa T.: "*Analog implementation of neo-fuzzy neuron and its on-board learning Computational Intelligence and Applications*", *Piraeus: WSES Press, 1999*

[27] A. Soualhi, A. Sari, H. Razik, P. Venet, G. Clerc, R. German, O. Briat, J.M. Vinassa: "*Supercapacitors ageing prediction by neural networks*". IECON 2013 (39th Annual Conference of the IEEE Industrial Electronics Society) Vienna, Austria, 2013, pp. 6812 – 6818.

[28] A. Soualhi, H. Razik, G. Clerc: "*Prognosis of Bearing Failures using Hidden Markov Models and the Adaptive Neuro-Fuzzy Inference System*". IEEE Transactions on IES, 2014, vol 61, n°6, pp. 2864-74.

[29] E. Niel, S. Zairi, H. Kadri, K. Quintero, « *Une co-modélisation pour l'évaluation de la fiabilité dynamique* », lambda Mu 2014, Dijon 21-23 octobre, 2014

[30] A. Avizienis, J.-C. Laprie, B. Randell, C. Landwehr: "*Basic Concepts and Taxonomy of Dependable and Secure Computing*", Dependable and secure computing (IEEE trans. on), 1 (1), 2004.

[31] G. Faraut, L. Piétrac, E. Niel: "*Formal Approach to Multimodal Control Design: Application to Mode Switching*", Industrial Informatics (IEEE trans. on), 5 (4), 2009.

[32] G. Faraut, L. Piétrac, E. Niel: "*Equivalence of behaviors between centralized and multi-model approaches*", International Conference on Automation Science and Engineering, Case, Trieste, 2011.

[33] Clarke, E.M.: "*25 years of model checking*", chapter The birth of model checking, 1–26. Springer-Verlag, Berlin, Heidelberg, 2008

[34] Marchand, H., Bournai, P., LeBorgne, M., and Guernic, P.L.: "*Synthesis of discrete-event controllers based on the SIGNAL environment*", in Discrete Event Dynamic Systems: Theory and Applications, 325–346, 2000

[35] Hajjar, S., Dumitrescu, E., Piétrac, L. and Niel, E.: "*A design method for synthesizing control-command systems out of reusable components*", Proceedings of the IFAC International Workshop of Discrete Event Sys- tems (WODES'14), 60–65. Cachan, France, 2014